THE JOURNAL OF PHYSICAL CHEMISTRY B
A JOURNAL OF THE AMERICAN CHEMICAL SOCIETY

pubs.acs.org/JPCB Article

Comprehensive Investigation of the Photophysical Properties of Alkynylcoumarin Gold(I) Complexes

Andrea Pinto, Carla Cunha, Gabriel Aullón, João Carlos Lima, Laura Rodríguez,* and J. Sérgio Seixas de Melo*

Cite This: https://doi.org/10.1021/acs.jpcb.1c07985 Read Online

ACCESS | Metrics & More | Article Recommendations | Supporting Information

ABSTRACT: Six gold(I) complexes (R_3P-Au-Coum) containing three different alkynylcoumarin chromophores (Coum) with different electron-donating and electron-withdrawing characteristics and two different water-soluble phosphines (PR_3 = PTA (a) and DAPTA (b)) have been synthesized (**1a,b**, unsubstituted coumarin; **2a,b**, 4-methyl substituted coumarin; **3a,b**, 3-chloro and 4-methyl substituted coumarin). A comprehensive study of the photophysical properties of the R_3P-Au-Coum, together with their propynyloxycoumarin precursors **1**−**3**, was performed in solution at room and low temperatures. Spectral and photophysical characteristics of the R_3P-Au-Coum essentially depend on the electronic characteristics of the propynyloxycoumarin ligand. The presence of the Au(I) atom was found to be responsible for an increase of the intersystem crossing, with triplet state quantum yield values, ϕ_T, ranging from ∼0.05 to 0.35 and high coumarin phosphorescence quantum yield values for derivatives **1** and **2**; fluorescence dominates the deactivation in derivatives **3**. Efficient singlet oxygen photosensitization was observed for the new compounds **3a,b**. From TDDFT calculations, the relevant HOMO and LUMO of the compounds, i.e., those involved in the transitions, are dominated by the frontier orbitals associated with the coumarin core. The Au(I)-phosphine structure introduces a new transition assigned to an intraligand transition involving the phosphine ligand, and π(C≡C) system, to the p orbitals of phosphorus and gold atoms.

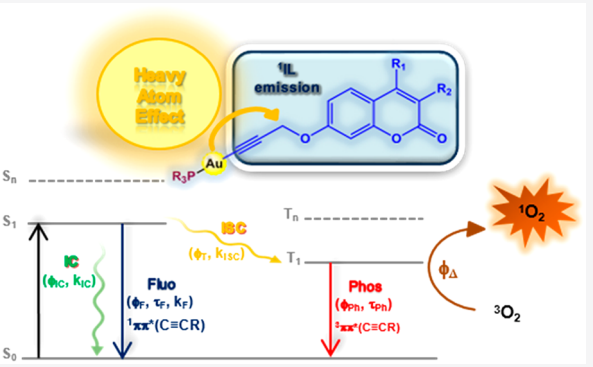

INTRODUCTION

During the past 2 decades the development of fluorescent organic materials has received much attention in various domains with applications in electronic displays, fluorescent switches, sensors, and optical devices.[1] Transition-metal complexes exhibit rich optical and luminescent properties, which can be enhanced and modulated through the metal centers with, among others, particular properties depending on the chemical configuration, the large variety of coordination numbers, and the presence of heavy atoms.[2−5]

The luminescence of gold(I) complexes is attributed in some cases to the aurophilic bonding, although a wide variety of electronic transitions have been reported, including intraligand and metal-centered transitions, ligand-to-metal and metal-to-ligand charge transfer (LMCT and MLCT, respectively), and of particular note, ligand-to-metal−metal bond charge transfer (LMMCT).[6−9]

The introduction of a gold(I) cation and the formation of the σ-bond between the carbon skeleton and the gold(I) ion can significantly modify the electronic states of an organic aromatic compound by enhancing spin−orbit coupling (SOC) interactions, thus increasing the rate of intersystem crossing (ISC, singlet−triplet transition $S_1 \rightarrow T_1$) relative to the pure organic chromophore, as well as the radiative rates between the lowest triplet states and the singlet ground state.[10] This leads to a rapid population of the triplet excited state and can further induce "forbidden" phosphorescence ($T_1 \rightarrow S_0$). This is the case, for example, of alkynyl-Au(I) derivatives, extensively explored in the past years, regarding their luminescent properties.[6] However, understanding the relationship between structure and photophysical properties in gold(I)-alkynyl remains limited. Therefore, of primary importance to the understanding of this relationship is the knowledge of the lifetimes, quantum yields, and rate constants for the all the deactivation processes. Only a few reports have been found to analyze the excited-state dynamics giving important information such as the effect of the organic chromophore and the nature of the bonding to the gold atom in the resulting very large intersystem crossing rate constants,[11,12] or the inclusion

Received: September 9, 2021
Revised: September 26, 2021

of a heteroatom to confer a strong intramolecular charge transfer character to the transitions as a possible reason for the close proximity of the k_{ISC} and k_{IC} values.[10,13] In fact, the presence of gold(I), as heavy atom, does not necessarily ensure a fast intersystem crossing rate, and the nature of the ligands also plays an important role in the excited-state dynamics and deactivation mechanisms.[14−16] Conversely, in the case of moderate intersystem crossing rate constant values, comparable with that of fluorescence deactivation, room temperature fluorescence/phosphorescence dual emission can be observed for this sort of gold compound.[6,14] Additionally, the electronic properties of the ancillary alkynyl substituents were shown to affect significantly the rate of the ISC process by means of altering the contribution of charge transfer transitions and therefore to influence the probability of singlet vs triplet emission.[17]

Efficient singlet oxygen sensitization and its evaluation from singlet oxygen quantum yields, ϕ_Δ, are other promising areas of research that have been poorly explored in the case of gold(I) complexes.[10,18−20] In fact, the well-known efficient SOC promoted by the presence of the gold(I) heavy atom makes these compounds particularly relevant to be investigated for applications in the fields of photodynamic therapy (PDT) or photocatalysis.[21]

There has been increasing interest over the past 20 years in organometallic complexes containing alkynyl units because of their potential application in many different fields, such as therapeutic drugs, photodynamic therapy agents, and sensors.[22−27] Within this field, Au(I) complexes represent an emerging area of investigation because of the structural characteristics of their ligands but also the presence of the heavy atom with direct effect on the resulting photophysical pathways.

In this work, we aim at studying the synthesis and characterization of a series of luminescent phosphane gold(I) alkynyl complexes containing an alkynyl-coumarin ligand with different electron-donating (methyl) or electron-withdrawing (chlorine) substituents (**1a**,**b**, **2a**,**b**, and **3a**,**b** in Scheme 1). It is

Scheme 1. Synthesis of Propynyloxycoumarin Ligands 1−3

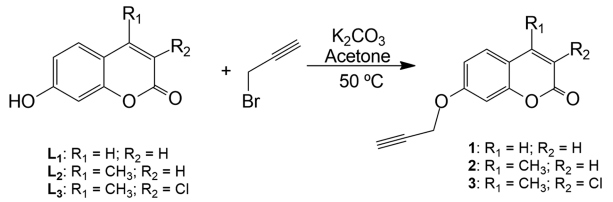

well-known that the photophysical properties of the coumarin derivatives can be tuned with the substituents and position in the coumarin ring.[28,29] Therefore, different coumarins bonded to the gold(I) atom through a propargyloxy group in the 7 position were chosen to investigate the effect of the substituents in the observed luminescent properties. Although some of the complexes were previously reported by some of us,[23] a detailed photophysical characterization is performed herein and the effect of the different electronic properties of the chromophore on the resulting photophysical parameters have been carefully analyzed, together with their potential as photosensitizers. Density functional theory (DFT) and time dependent DFT (TDDFT) studies have also been carried out to rationalize the observed experimental studies and to correlate their structural and photophysical properties.

EXPERIMENTAL SECTION

General Procedures. All manipulations have been performed under prepurified N_2 using standard Schlenk techniques. All solvents have been distilled from appropriated drying agents. Commercial reagents were 1,3,5-triaza-7-phosphatricyclo[3.3.1.13.7]decane (PTA, Aldrich 97%), 3,7-diacetyl-1,3,7-triaza-5-phosphabicyclo[3.3.1]nonane (DAPTA, Aldrich 97%), copper(I) chloride (Aldrich, 99%). Literature methods have been used to prepare [AuCl(PR_3)] (PR_3 = PTA,[30] DAPTA[31]), **1**,[23] **2**,[23] **1a**,[23] **1b**,[23] **2a**,[23] **2b**,[23] and **3**.[32]

All solvents used were of spectroscopic grade. Acetonitrile was purchased from Sigma-Aldrich. Deoxygenation was done by bubbling the solutions with a stream of argon or nitrogen for approximately 20 min in a device elsewhere described.[33] All measured solutions were freshly prepared (within the day) unless noted otherwise.

Physical Measurements. Infrared spectra have been recorded on a FT-IR 520 Nicolet spectrophotometer. ^{1}H NMR (δ(TMS) = 0.0 ppm) and ^{31}P NMR (δ(85% H_3PO_4) = 0.0 ppm) spectra have been obtained on Varian Mercury 400 and Bruker 400 (Universitat de Barcelona) instruments. Electrospray mass spectra (+) have been recorded on a Fisons VG Quatro spectrometer (Universitat de Barcelona). Absorption spectra were obtained in a 5 mm or 10 mm quartz cuvette in acetonitrile on a Cary 5000 UV−vis−NIR or Shimadzu UV-2450 spectrophotometer. The emission spectra of the compounds in solution were obtained in a fluorescence quartz cuvette of 5 mm or 10 mm path length, using a Horiba-Jobin-Vonn Fluorolog 3.22 or Fluoromax spectrometers. Phosphorescence spectra and decays were obtained with the D1934 unit of Fluoromax 3.22 spectrometer. All the fluorescence and phosphorescence spectra were corrected for the wavelength response of the system with the appropriate correction files obtained for the instrument.

Emission Quantum Yield Determination and Laser Flash Photolysis Experiments. All measured solutions were degassed using a cuvette especially designed and described elsewhere for 20−30 min with N_2 or Ar.[33] Emission quantum yields of the compounds were determined with a Hamamatsu Quantaurus QY absolute photoluminescence quantum yield spectrometer model C11437 (integration sphere). Transient absorption spectra were measured using a flash photolysis setup composed of a LKS 60 ns laser photolysis spectrometer from Applied Photophysics, with a Brilliant Q-switch Nd:YAG laser from Quantel, using the fourth harmonics (λ_{exc} = 266 nm, laser pulse half-width equal to 6 ns). The transient spectra were obtained by monitoring the optical density change at 5−10 nm intervals, averaging at least 10 decays at each wavelength.

The triplet yields (ϕ_T) of the compounds were measured by the singlet depletion method, eq 1,[34] using benzophenone as the reference actinometer:

$$\phi_T = \phi_{T_{std}} \frac{\Delta OD_{cp}}{\Delta OD_{ref}} \frac{\varepsilon_{T_{std}}}{\varepsilon_T} \quad (1)$$

where ref stands for the reference solution containing benzophenone (ϕ_T = 1; $\varepsilon_{T_{std}}$ = 6500 cm^{-1} M^{-1}) in acetonitrile, optically matched with the sample solution at 266 nm (**1a**,**b** and **2a**,**b**) and at λ_{exc} = 355 nm (**3a**,**b**).

https://doi.org/10.1021/acs.jpcb.1c07985
J. Phys. Chem. B XXXX, XXX, XXX−XXX

Singlet Oxygen Yields. Room-temperature singlet oxygen phosphorescence was detected at 1270 nm with a Horiba-Jobin-Ivon SPEX Fluorog 3.22 using the Hamamatsu R5509-42 photomultiplier previously reported. The use of a Schott RG1000 filter was essential to eliminate from the infrared signal all of the first harmonic contributions of sensitizer emission in the region below 850 m. The singlet oxygen formation quantum yield was then determined by direct measurement of the phosphorescence at 1270 nm following irradiation of the aerated solution of the samples in acetonitrile. 1*H*-Phenal-1-one in acetonitrile (ϕ_Δ = 0.98) was used as standard,[35] applying eq 2.

$$\phi_\Delta = \phi_\Delta^{ref} \frac{\text{Emission}_{1270nm}}{\text{Emission}_{1270nm}^{ref}} \quad (2)$$

with ϕ_Δ^{ref} being the singlet oxygen formation quantum yield of the reference compound. 1*H*-Phenal-1-one in acetonitrile (ϕ_Δ = 0.98) was used as the standard.

Time-Resolved Fluorescence (TCSPC). Fluorescence decays were measured by using a home-built picosecond time-correlated single photon counting (TCSPC) apparatus describe in detail elsewhere.[36] Shortly, excitation was performed with the third harmonic at 275 nm (generated with a Spectra Physics GWU-23PS module) from a picosecond Spectra Physics mode-lock Tsunami laser (Ti:sapphire) model 3950 (80 MHz repetition rate, tuning range 700−1000 nm), pumped by a Millennia Pro-10s continuous wave, solid-state laser (532 nm). A double subtractive Oriel Cornerstone 260 monochromator and a Hamamatsu microchannel plate photomultiplier (R3809U-50) were used for the selection of the emission wavelength and signal detection, respectively. The signal acquisition and data processing are performed with a Becker and Hickl SPC-630 TCSPC module. The fluorescence decays and the instrumental response function (IRF) were collected using 1024 channels in time scales varying from 3.26 to 6.4 ps/channel scale, until 2000−5000 counts at maximum were reached. The full width at half-maximum (fwhm) of the IRF was 25 ps. Deconvolution of the fluorescence decay curves was performed using the modulating function method as implemented by Striker et al. in the SAND[37] program which allows a value of ∼10% of the fwhm (∼2 ps) as the time resolution of the equipment with this excitation source.

Theoretical Calculations. Density functional calculations were carried out using the Gaussian 09 package.[38] The hybrid density functional known as B3LYP was applied.[39,40] Effective core potentials (ECPs) were used to represent the innermost electrons of the gold atom and the basis set of valence triple-ζ quality with an extra d-polarization function.[41] A similar description was used for all main group elements.[42] Atomic charges and populations analysis have been confirmed from natural populations analysis (NPA).[43] Solvent effects of acetonitrile were taken into account by PCM calculations,[38] keeping the optimized geometries for the gas phase without symmetry restrictions. Excited states and absorption spectra were obtained from the time-dependent density functional theory (TD-DFT) implemented in Gaussian 09.[44] In addition and to account for possible significant solvent effects, two model compounds (**2a** and **3a**) have been reoptimized in solution (PCM calculations using the SMD model), followed by time-dependent calculations including solvent effects, and the results obtained were practically identical to those obtained with the optimized molecules in the gas phase. Moreover, the phosphorescence emission for **2a** does not change when including solvent effects, while a decrease of a few nm is found for **3a** due to a higher stabilization, of 0.6 kcal/mol, for the unrelaxed state S_0*.

Synthesis and Characterization. The organic alkynyl ligands have been prepared following the method previously reported by us (Scheme 1).[23] The commercial hydroxycoumarins $\mathbf{L_1}$−$\mathbf{L_3}$ were reacted with propargyl bromide in acetone at 50 °C in the presence of K_2CO_3. The corresponding propynyloxycoumarins **1**−**3** were obtained in high yields (∼75%) after 18−36 h of stirring under reflux and after purification by column chromatography.

The deprotonation of the terminal alkynyl proton of **1**−**3** with a KOH methanol solution and addition of a stoichiometric quantity of [AuCl(PR_3)] (PR_3 = PTA or DAPTA) complexes in dichloromethane give rise to the formation of the neutral propargyloxycoumarin phosphine gold(I) complexes **1**−**3a** and **1**−**3b** (containing PTA and DAPTA phosphine, respectively) as depicted in Scheme 2. We previously described compounds **1a,b** and **2a,b**, and comparison with the recorded spectroscopic data indicates their correct formation in pure form (Figures S1 and S2).[23]

Scheme 2. Synthesis, Structures, and Acronyms of the Propargyloxycoumarin Phosphine Gold(I) Complexes 1a−3a and 1b−3b

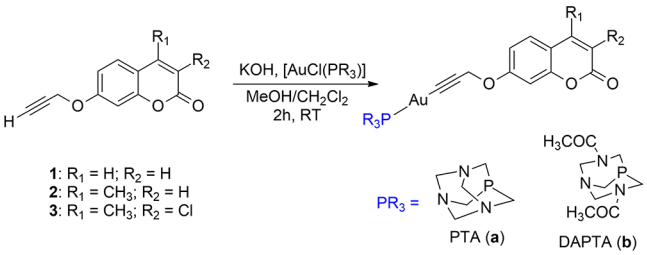

Characterization of the complexes **3a,b** by ^{1}H and ^{31}P NMR and IR spectroscopy and ESI(+) mass spectrometry indicates the successful formation of the complexes. A direct evidence of the successful preparation of the complexes is the disappearance of the terminal alkynyl hydrogen, and this is clearly observed in the corresponding IR and ^{1}H NMR spectra of the gold(I) complexes. The hydrogen atoms of the phosphines follow the typical patterns of PTA (Figure S3) and DAPTA (Figure S6). ^{31}P NMR shows a ∼10 ppm downfield shift with respect to the AuClPR_3 precursors, as observed for other similar compounds (Figures S4 and S7).[25,10,23,45−47] Moreover, molecular peaks have also been obtained by ESI(+) mass spectrometry displaying the $[M + H^+]^+$ peak for all the species (see Figures S5 and S8).

RESULTS AND DISCUSSION

Electronic Spectral Characterization. Figure 1 depicts the absorption and fluorescence emission and excitation spectra of the gold(I) complexes (**1a,b**, **2a,b**, and **3a,b**) together with the different propynyloxycoumarin ligands (**1**−**3**) in acetonitrile at room temperature (293 K) and the phosphorescence ($T_1 \rightarrow S_0$) emission in 2-methyltetrahydrofuran (2-MeTHF) at low temperature (77 K). The overlap between absorption and excitation spectra further confirms the purity of the synthesized compounds, beyond the level accessible by NMR spectroscopy. Electronic spectral data

https://doi.org/10.1021/acs.jpcb.1c07985
J. Phys. Chem. B XXXX, XXX, XXX−XXX

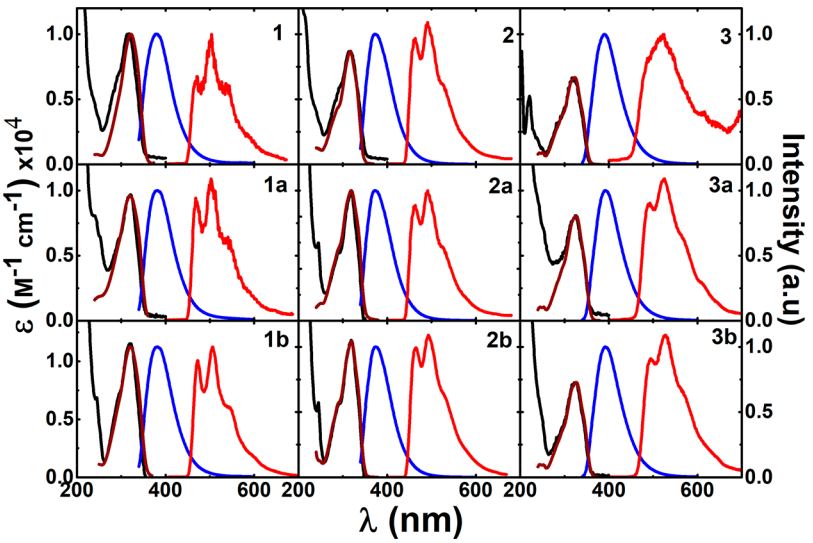

Figure 1. Electronic absorption (black line), fluorescence emission (blue line), and excitation (wine line) spectra in acetonitrile at T = 293 K (at λ_{exc} = 320 nm) together with the phosphorescence emission (red line) spectra in 2-MeTHF, at T = 77K, of gold(I) complexes and respective ligands. Concentration of the samples is equal to 1.3 × 10^{-5} M.

Table 1. Spectral Data (Including Wavelength Absorption, λ_{abs}, Fluorescence Emission Maxima ($\lambda_{max}^{Fluo}(S_1 \rightarrow S_0)$), ν_{00} Frequency (cm^{-1}), and Stokes' Shift, Δ_{ss} (cm^{-1})) for the Gold(I) Complexes and Respective Alkynylcoumarin Precursors in Acetonitrile (MeCN) at Room Temperature (293 K), Maximum Phosphorescence Emission ($\lambda_{max}^{phosp}(T_1 \rightarrow S_0)$) in 2-Methyltetrahydrofuran (2-MeTHF) at Low Temperature (77 K), and Transient ($\lambda_{max}^{abs}(T_1 \rightarrow T_n)$) Maxima

compd	λ_{abs} (nm)	$\lambda_{max}^{Fluo}(S_1 \rightarrow S_0)$ (nm), (ν_{00} (cm^{-1}))	$\lambda_{max}^{abs}(T_1 \rightarrow T_n)$ (nm), (ν_{00} (cm^{-1}))	Δ_{ss} (cm^{-1})	$\lambda_{max}^{phosp}(T_1 \rightarrow S_0)$ (nm)
1	316	381, (26247)	N.O.[a]	5399	504
1a	320	381, (26247)	480, (5414)	5003	503
1b	321	381, (26247)	480, (5414)	4906	507
2	316	374, (26738)	N.O.[a]	4908	489
2a	318	373, (26810)	480, (5977)	4637	491
2b	318	374, (26738)	480, (5905)	4709	493
3	323	390, (25641)	N.O.	5319	524
3a	325	393, (25445)	480, (4612)	5324	525
3b	328	392, (25510)	480, (4677)	4978	528

[a]N.O.: not observed.

(wavelength maxima for absorption, fluorescence, and phosphorescence emission, Stokes shift, and transient maxima, $T_1 \rightarrow T_n$) are summarized in Table 1. The ν_{00} ($0' \rightarrow 0$ energy for the S_1 and T_1 states) was obtained from the fluorescence emission spectra obtained at 293 K in acetonitrile and the phosphorescence spectra at 77 K in 2-MeTHF (Table 1). Photophysical data (including quantum yields, lifetimes, and rate constants for the singlet and triplet deactivation and formation processes) are summarized in Table 2.

As previously observed for **1a,b** and **2a,b** derivatives in methanol, the absorption and emission spectra of the Au(I) complexes are basically identical to those of their alkynylcoumarin precursors (Figure 1). Thus, these spectral properties (band shape and position) are essentially dependent on the alkynylcoumarin ligand, i.e., intraligand electronic transitions.[23] This is further confirmed with TDDFT theoretical calculations where the relevant transitions are located in the coumarin core (see TDDFT calculation discussion below).

The presence of one absorption band between 315 and 330 nm (Figure 1) is consistent with the $\pi-\pi^*$ absorption transition of the coumarin chromophoric unit (intraligand transitions), and the fluorescence coumarin emission is observed, for all compounds, at approximately 370−395 nm.[28,29]

The effect of the substituents on the coumarin core is also clearly evidenced in the luminescence properties. A general trend can be observed where the absorption and emission wavelengths are red-shifted in the order **2**, **2a,b** < **1**, **1a,b** < **3**, **3a,b** indicating that the presence of only an electron-donating substituent (**2** derivatives) induces a blue-shift of the bands that is equilibrated by the electron-withdrawing character of the chlorine substituent in **3**, modifying the transition energy value (see below TDDFT calculations discussion). Interestingly, the presence of an electron-withdrawing group, chlorine, at the 3-position in organic ligand **3** and the corresponding new Au(I) complexes (**3a,b**) affects both the luminescent quantum yields and lifetimes, with a significant increase being recorded for both parameters (see Table 2).

Luminescence spectra carried out at 77 K display a vibronically structured band centered at 490−530 nm, found independent of the excitation wavelength and is attributed to a $^3\pi,\pi^*$ state which is localized on the coumarin chromophoric (see Figure 1 and Table 1). We observe virtually no fluorescence band; the lower-lying emission is attributed to a triplet-excited state (phosphorescence, $T_1 \rightarrow S_0$) due to

https://doi.org/10.1021/acs.jpcb.1c07985
J. Phys. Chem. B XXXX, XXX, XXX−XXX

Table 2. Photophysical Properties Including Quantum Yield (Fluorescence, ϕ_F, Phosphorescence, ϕ_{ph}, Singlet Oxygen Sensitization, ϕ_Δ, Intersystem Crossing, ϕ_T, and Internal Conversion, ϕ_{IC}), Lifetimes (τ_F, τ_{ph}, and τ_T) and Rate Constants (k_F, k_{NR}, k_Q, k_{IC}, and k_{ISC}) Obtained in Aerated (with O_2) or Degassed (N_2 sat.) Acetonitrile Solutions at 293 K and 77K for the PTA-Au-Coum (1a–3a), DAPTA-Au-Coum (1b–3b), and the Parent Compounds (1–3)

compd	ϕ_F (with O_2), 293 K	ϕ_F (N_2 sat.), 293 K	ϕ_F, 77 K	ϕ_{ph}, 77 K	$\phi_F + \phi_{ph}$, 77 K	τ_F (ns), 293 K	τ_{ph} (s), 77 K	τ_T (μs), 293 K	ϕ_Δ	ϕ_T	ϕ_{IC} [b]	k_F (ns^{-1}) [b]	K_{NR} (ns^{-1}) [b]	$k_Q \times 10^9$ (s^{-1})	k_{IC} (ns^{-1}) [b]	k_{ISC} (ns^{-1}) [b]
1	0.008	0.011	0.621	0.048	0.669	0.012	0.77	N.O.[a]	N.O.[a]	N.O.[a]	N.O.[a]	0.7	83	N.O.[a]	N.O.[a]	N.O.[a]
1a	0.01	0.011	0.578	0.134	0.712	0.032	0.68	40	0.04	0.05	0.94	0.3	31	5.33	29.4	1.6
1b	0.011	0.012	0.558	0.133	0.691	0.038	0.65	10	0.04	0.35	0.64	0.3	26	28.2	16.8	9.2
2	0.013	0.016	0.677	0.198	0.875	0.035	1.06	N.O.[a]	N.O.[a]	N.O.[a]	N.O.[a]	0.4	28	N.O.[a]	N.O.[a]	N.O.[a]
2a	0.024	0.025	0.406	0.347	0.753	0.084	0.84	26	0.06	0.31	0.67	0.3	12	32.7	7.9	3.7
2b	0.03	0.032	0.539	0.461	1	0.078	0.74	15	0.07	0.24	0.73	0.4	12	37.6	9.4	3.1
3	0.613	0.666	0.975	0.044	1	2.15	0.224	N.O.[a]	N.O.[a]	N.O.[a]	N.O.[a]	0.3	0.2	N.O.[a]	N.O.[a]	N.O.[a]
3a	0.658	0.711	0.628	0.058	0.686	2.36	0.145	34	0.12	0.11	0.23	0.3	0.1	5.32	0.10	0.05
3b	0.665	0.728	0.52	0.048	0.568	2.5	0.154	37	0.18	0.24	0.10	0.3	0.1	2.48	0.04	0.10

[a]N.O.: not observed. [b]$\phi_{IC} = 1 - (\phi_F + \phi_T)$; $k_F = \frac{\phi_F}{\tau_F}$; $k_{NR} = \frac{(1-\phi_F)}{\tau_F}$; $k_{IC} = \frac{1-\phi_T-\phi_F}{\tau_F}$; $k_{ISC} = \frac{\phi_T}{\tau_F}$.

substantial Stokes shift measured and the longer excited state lifetime. This is further confirmed from ns-TA data and TDDFT calculations (see below). The heavy atom effect brought about by the Au(I) unit facilitates the intersystem crossing so that phosphorescence can be readily measured. In the case of **1**, **2**, and **3**, the quantum yield for triplet formation is too low to be accurately measured by transient absorption (Tables 1 and 2), but at 77 K it can be seen that all ligands display phosphorescence, even if of lower intensity than the complexes. Fluorescence and phosphorescence lifetimes, quantum yields, and rate constants results for the alkynyl gold(I) complexes, obtained from the measured fluorescence and triplet state formation quantum yields and singlet state decay times, are summarized in Table 2. The values obtained for previously studied propynyloxycoumarin ligands are again included for comparison.

The ϕ_{Ph} values for the propynyloxycoumarin ligands are 2–3 times lower than those of the corresponding gold(I) complexes except for compound **3**, whose value is barely affected relative to **3a**,**b**. The ϕ_{Ph} values of **1**, **1a**,**b** and **2**, **2a**,**b** collected at 77 K are found between 0.65 and 1.06 s, while the corresponding values for the chlorine derivatives **3** and **3a**,**b** are ~0.15 s. The observed differences are indicative of the clear effect of the electron-withdrawing substituent in the resulting photophysical parameters, favoring less the intersystem crossing and corresponding phosphorescence processes, in agreement with the lower ϕ_{Ph} values and higher quantum yields of singlet oxygen sensitization (ϕ_Δ); see Table 2. The ϕ_Δ values obtained for the gold(I) complexes are higher for those containing DAPTA (**1c**, **2c**, and **3c**) than those containing the PTA (**1b**, **2b**, and **3b**) phosphine. The highest ϕ_Δ values are recorded for the new chlorine derivatives (**3a**,**b**), with efficiencies ranging from 12% to 18%. Additionally, the sum of the fluorescence and phosphorescence quantum yields ($\phi_F + \phi_{Ph}$) is, at low temperature of 77 K, relatively high: always above 57% and in the cases of **2b** and **3** equals 1; see Table 2. This shows that at low temperature, the radiative emission dominates the deactivation processes with particular emphasis in compounds **2b** and **3**. Moreover, comparison of the fluorescence and phosphorescence quantum yields clearly shows the effect of the heavy atom on the increase of the conversion from singlets to triplets (increase of spin–orbit coupling, SOC, contributions due to the heavy atom effect promoted by gold).

ns-Transient Absorption. Time-resolved transient absorption spectra in the ns-TA were obtained in order to get further insights into the characteristics of the formed excited states. The transient triplet–triplet absorption spectra of the Au(I) complexes were recorded by laser flash photolysis at 266 nm (ns-TA) of degassed acetonitrile solutions and are depicted in Figure 2. The spectra display an intense and broad triplet–triplet absorption ranging between 400 and 550 nm, together with depletion (ground-state bleaching) below 350 nm consistent with the ground-state absorption of these compounds. Inspection of the spectra at room temperature, together with the data summarized in Table 1, shows that the wavelength maxima of the triplet–triplet transient are basically constant for the six Au(I) complexes (**1a**,**b**, **2a**,**b**, and **3a**,**b**) at around ~480 nm and the triplet lifetimes are in the range ϕ_T = 10–40 μs; see Table 2.

Rate Constants for the Excited State Deactivation Processes. The relevant rate constants for the deactivation of the lowest lying singlet and triplet excited states are

https://doi.org/10.1021/acs.jpcb.1c07985
J. Phys. Chem. B XXXX, XXX, XXX–XXX

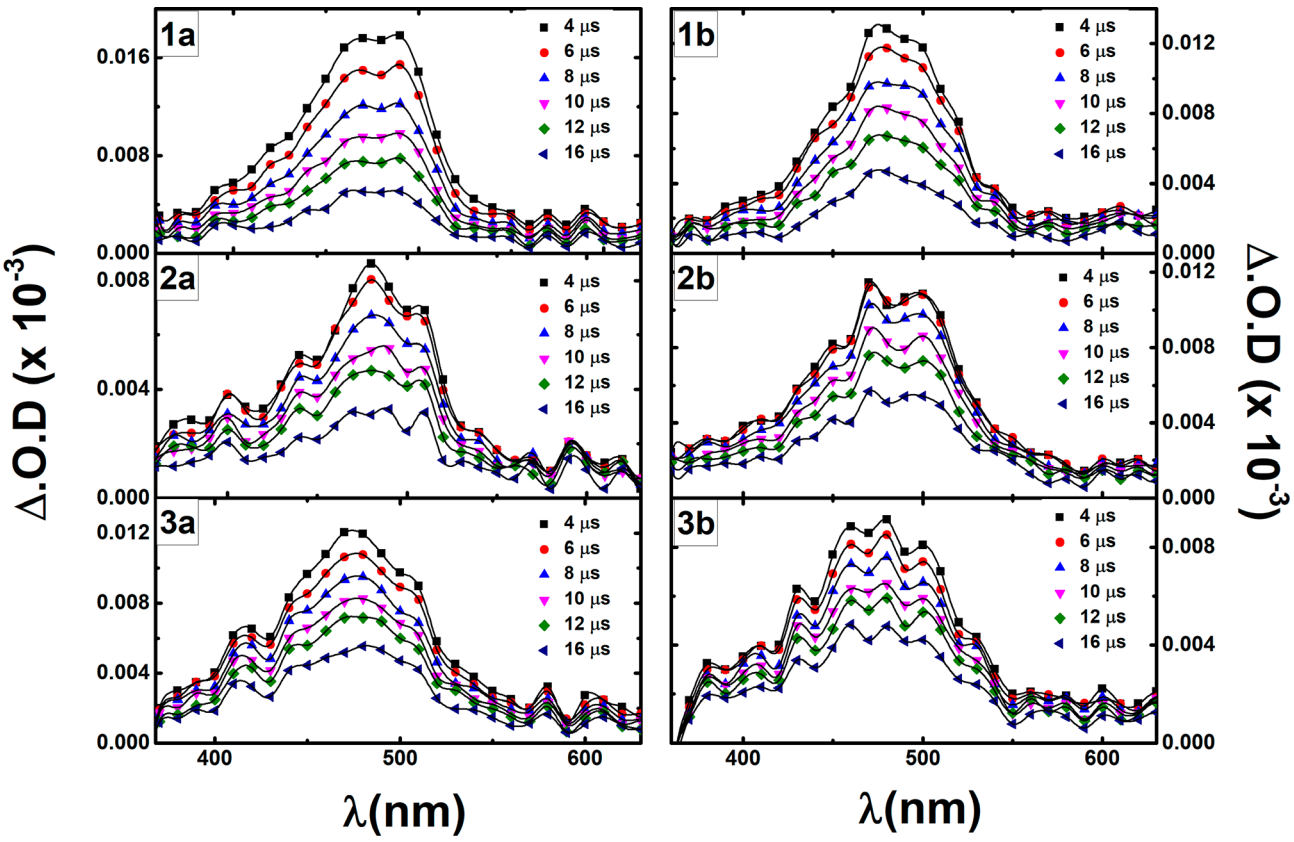

Figure 2. Room temperature time-resolved transient triplet−triplet absorption spectra (ns-TA) for gold(I) complexes (**1a,b**, **2a,b**, and **3a,b**) obtained by laser flash photolysis with excitation at 266 nm in degassed acetonitrile solutions.

summarized in Table 2, from where it can be seen that despite the presence of the gold atom, the dominant deactivation pathway is, for all compounds, the radiationless $S_1 \rightsquigarrow S_0$ internal conversion, k_{IC}.

Rate constants for the energy transfer from the gold complexes to the molecular oxygen were obtained from eq 3,

$$k_Q = \left(\frac{1}{\tau_T} - \frac{1}{\tau_T^0}\right) \times \frac{1}{[Q]} \quad (3)$$

where τ_T^0 is the triplet lifetime in the absence of oxygen and ϕ_T in the presence of oxygen and [Q] is the concentration of the quencher, oxygen.

The values of the rate constants, k_Q, in Table 2 are in the order of 10^{10} s^{-1} and are slightly higher (in the range 2.5×10^9 to 38 L mol^{-1} s^{-1}) than pure controlled diffusion reaction rates in this solvent (k_{diff} = 1.9×10^{10} L mol^{-1} s^{-1}). This may indicate that the process is not purely diffusional and that ground-state interaction may exist between molecular oxygen and the Au(I) complex which increases the rate of the energy transfer process.

Moreover, the values of the radiative (k_F) and nonradiative (k_{NR}) rate constants for the gold complexes indicate that the first is kept approximately constant for all compounds with values ranging from 0.3 to 0.4 ns^{-1}, whereas the radiationless decay pathway is dominant in all Au(I) complexes. The exception is found for the chlorine derivatives (**3**, **3a**,**b**) where k_{NR} is 2 orders of magnitude lower than with all the others compounds (Table 2). Indeed, the phosphine (PTA or DAPTA) does not seem to introduce appreciable changes in the photophysical parameters of **3**, **3b**, and **3c**, where the radiative route dominates the excited state deactivation.

TD-DFT Theoretical Studies. The different molecular geometries have been optimized by DFT calculations, and the main transitions expected for both absorption and emission have been analyzed. Similar geometries for all coumarin groups are predicted in both the ligands and corresponding complexes although the C≡C bond is found to be slightly weaker in the gold(I) derivatives (1.20 Å in **1a,b**, **2a,b**, and **3a,b** vs 1.21 Å in **1**−**3**).

The UV−vis spectra of the ligands are practically identical with a band centered at ∼310 nm in acetonitrile ($\varepsilon \sim 20\,000$ $M^{-1}\cdot cm^{-1}$) corresponding to a $\pi-\pi^*$ transition within the coumarin (Table S1) and slightly higher than the values found in the literature for the correspondent methoxycoumarin in cyclohexane.[28,29] In the case of coumarin a lowest lying S_1 state of n,π^* was predicted from both theory and experiment, yet buried underneath the strong S_2 state of $\pi-\pi^*$ origin.[29] Moreover, the following trend is observed in the absorption wavelength, 305 (**2**) < 308 (**1**) < 317 (**3**), in agreement with the experimental data in Table 1 and Figure S9. This is due to the modification in the HOMO−LUMO energy gap, which is affected by the substituents at the 3 and 4 positions of the coumarin rings (Figure S10).

Absorption spectra for the gold(I) complexes reproduce the same trends of the related organic counterparts, being indicative of the main role of the substituents at the coumarin in the photophysical properties (Figures S11−S17). The transition at 310−320 nm is also located in the coumarin rings, but a 3−4 nm red-shift is predicted for the gold(I) complexes, in agreement with the experimental data, together

https://doi.org/10.1021/acs.jpcb.1c07985
J. Phys. Chem. B XXXX, XXX, XXX−XXX

Table 3. Calculated Absorption Parameters (Wavelengths in nm and Their Intensities in Parentheses) for the Coumarin Derivatives in Acetonitrile Solution

assignment	compd	1	2	3
coumarin: π(Cou) → π*(Cou)		308 (0.47)	305 (0.44)	317 (0.49)
	a	312 (0.57)	307 (0.46)	320 (0.57)
	b	312 (0.57)	308 (0.46)	320 (0.59)
				247 (0.10)
intraligand: π(CC) → PTA + p(Au)	**a**	263 (0.27)	262 (0.27)	263 (0.28)
	b	237 (0.14)	237 (0.18)	237 (0.19)

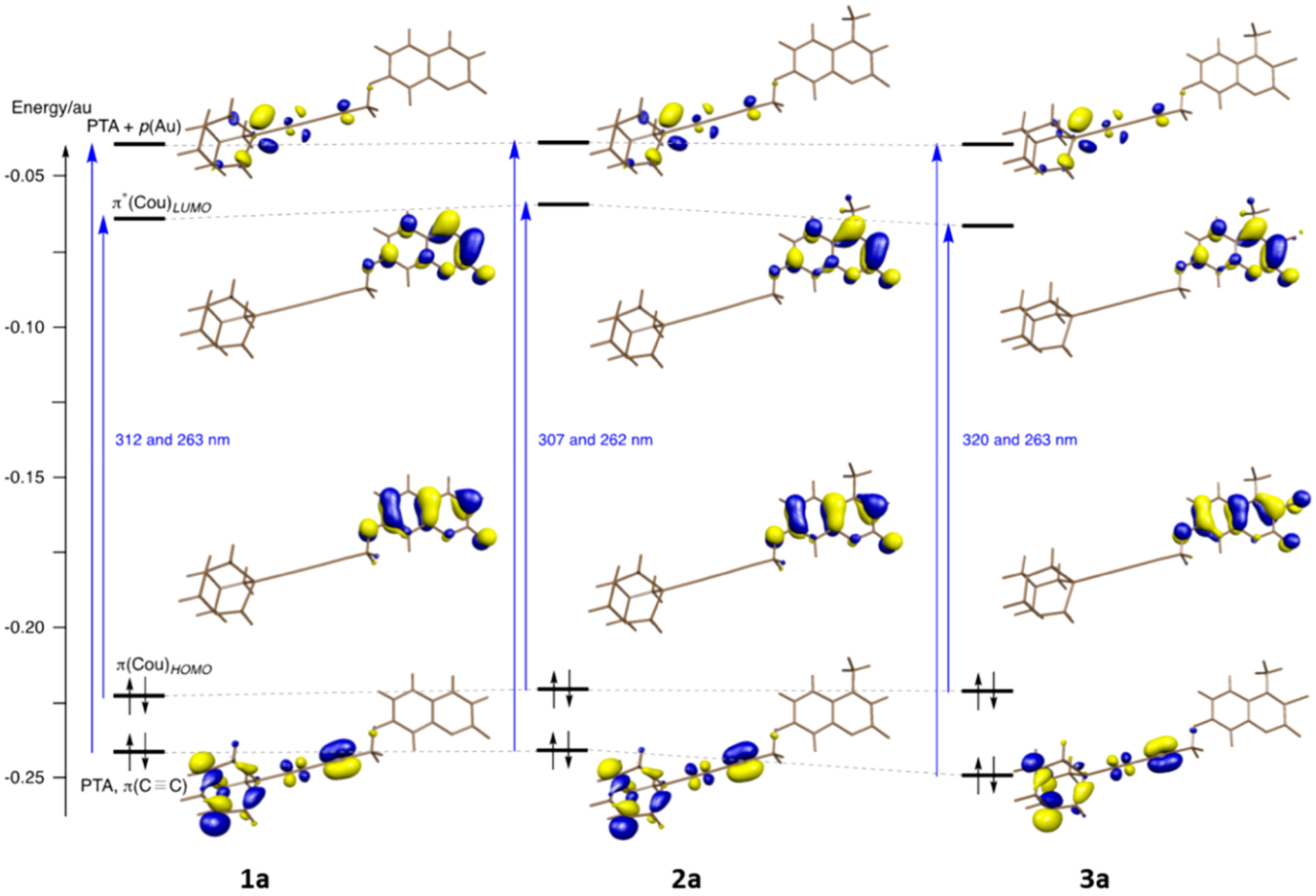

Figure 3. Schematic representation of the main expected transitions in the absorption spectra of PTA-Au-Coum complexes with coumarins (**1a**–**3a**).

with an increase of the theoretically calculated ε values to ~25 000 $M^{-1}\cdot cm^{-1}$. However, the gold(I)-phosphine framework participates in the absorption spectra by the introduction of a new transition at 263 and 237 nm (for **1**–**3a** and **1**–**3b** complexes respectively; see Table S2). The analysis of the involved orbitals allows us to assign to an intraligand transition having monoexcitations from the phosphine ligand and π(C≡C) system toward p orbitals of phosphorus and gold atoms (Table 3 and Figures 3 and 4).

In an attempt to understand the phosphorescent properties of the coumarin derivatives, emission, geometries for the first triplet state were optimized. The calculated energies for the triplet state of the propynyloxycoumarin ligands (**1**–**3**) are basically identical to the values of the corresponding gold(I)-coumarin complexes (**1a**,**b**, **2a**,**b**, and **3a**,**b**) thus showing that the energy of these triplet states is practically independent of the complexation with the Au(I) and essentially localized in the propynyloxycoumarin ligands (Table 4). As example, a phosphorescence emission is predicted at approximately 575–577 nm for **1** and **1a**,**b**, 556–559 nm for **2** and **2a**,**b**, and 648–653 nm for **3** and **3a**,**b**.

The lower phosphorescence yields displayed by the 3-chlorocoumarin derivatives (**3**, **3a**,**b**) relative to the other compounds (**1**, **1a**,**b** and **2**, **2a**,**b**) have led to additional investigations. A detailed analysis of the optimized geometries reveals dramatic structural changes in the lactone ring of the coumarin core. Indeed, according to the molecular diagram, excitation of an electron from HOMO to LUMO provides a lengthening of the distance between the C3 and C4 atoms (see Table S3), further corroborated by the increase from 1.35 to 1.45 Å in singlet and triplet states respectively, resulting in lower variations for other distances. Although in all cases these atoms remain in a planar environment, a significant deformation of the lactone ring, $\theta(C^4\cdot O^1)$, is observed, being

https://doi.org/10.1021/acs.jpcb.1c07985
J. Phys. Chem. B XXXX, XXX, XXX–XXX

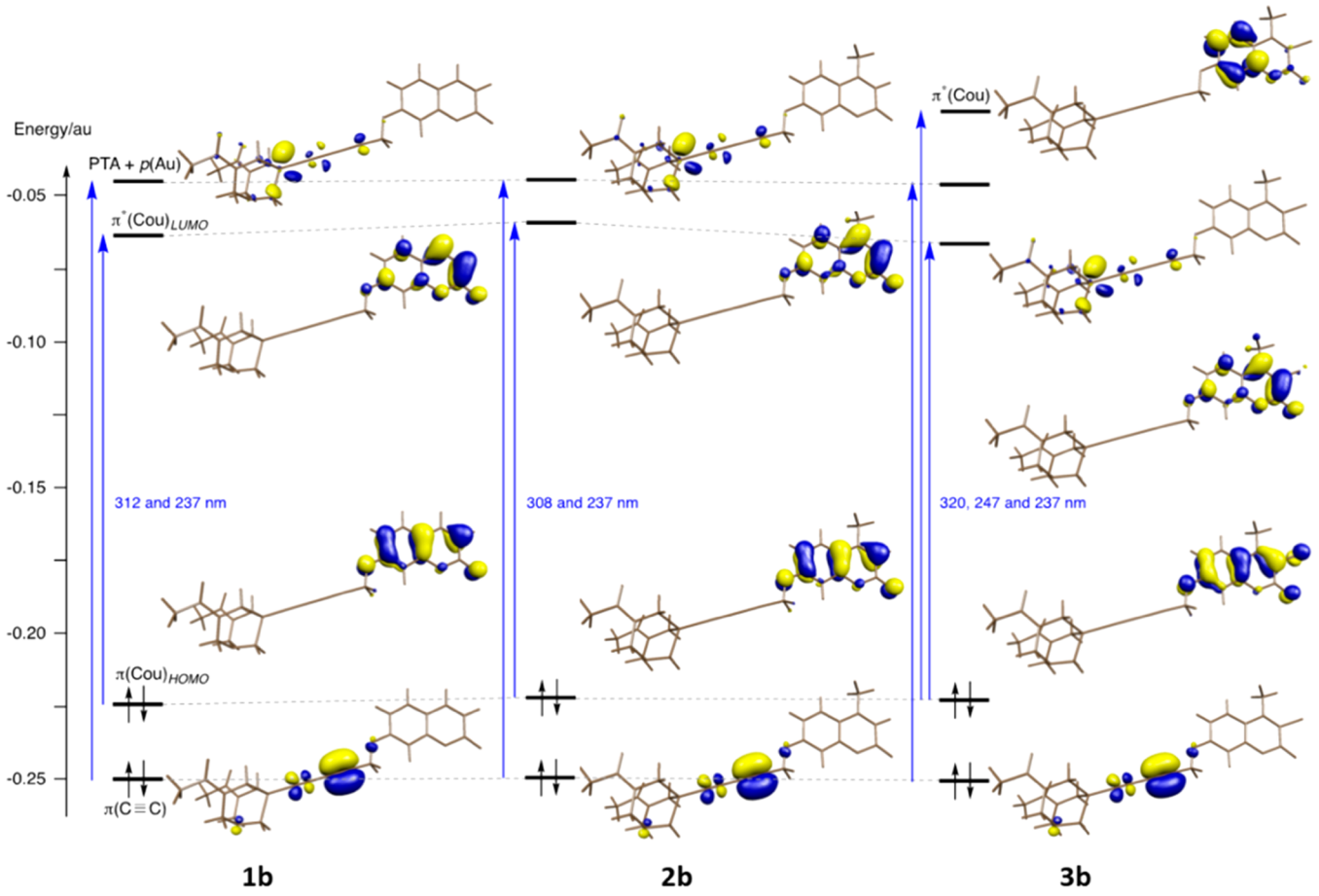

Figure 4. Schematic representation of the main expected transitions in the absorption spectra of DAPTA-Au-Coum complexes with coumarins (**1b**−**3b**).

Table 4. Calculated Energies for Optimized Triplet State T_1, Relative Energy (in eV, and nm in Parentheses and in the Franck−Condon Geometry) from the Ground State S_0 in Acetonitrile Solution, and Phosphorescence Emission ($T_1 \rightsquigarrow S_0$), from the Relaxed Geometry

compd	T_1[a]	emission, eV[a]	$\theta(C^4{\cdot}O^1)$
1	2.62 (473)	2.15 (577)	179.9
1a	2.61 (475)	2.16 (575)	180.0
1b	2.61 (475)	2.16 (575)	179.8
2	2.70 (459)	2.22 (559)	179.7
2a	2.69 (461)	2.23 (556)	179.2
2b	2.69 (460)	2.23 (556)	179.7
3	2.53 (489)	1.90 (653)	165.7
3a	2.53 (491)	1.91 (649)	165.1
3b	2.53 (490)	1.91 (648)	165.1

[a]In parentheses, values in nm.

practically planar in families **1** and **2** while it is even bent across antipodal atoms C4 and O1 in **3**. Consequently, a major structural arrangement is needed to involve triplet states in the chlorine derivatives, even low gap is calculated, and therefore we would suggest that this is the reason for mainly fluorescence emission (see Table S4).

CONCLUSIONS

The synthesis and a comprehensive photophysical characterization were undertaken for six luminescent propargyloxycoumarin phosphine gold(I) complexes (**1a**,**b**, **2a**,**b**, and **3a**,**b**). The absorption, emission and phosphorescence spectra of PR_3-Au-Coum (PR_3 = PTA (a) and DAPTA (b)) complexes are found to be very similar to the propynyloxycoumarin ligands (**1**−**3**). In contrast with the coumarin counterparts, where the internal conversion dominates the excited state deactivation, with the Au(I) complexes, competition with $S_1 \rightsquigarrow T_1$ intersystem crossing is found. The overall experimental and theoretical data show that the excited state is mainly located in the propynyloxycoumarin ligand. With compounds **3a**,**b**, containing an electron-withdrawing group, chlorine, at the 3-position, the dominance of the radiative decay is not affected by the gold atom. Finally, and very promising, the triplet state is found to efficiently sensitize molecular oxygen with ϕ_Δ values ranging from 12% to 18% for the chloro derivatives **3a**,**b**.

ASSOCIATED CONTENT

Supporting Information

The Supporting Information is available free of charge at https://pubs.acs.org/doi/10.1021/acs.jpcb.1c07985.

^{1}H and ^{31}P NMR and ESI-MS(+) spectra of the compounds, representation of the minimum energy geometry conformation, orbital and coordinates involved in the transitions, and calculated UV−visible spectra of the different coumarins and gold(I) complexes (PDF)

https://doi.org/10.1021/acs.jpcb.1c07985
J. Phys. Chem. B XXXX, XXX, XXX−XXX

AUTHOR INFORMATION

Corresponding Authors

Laura Rodríguez − *Departament de Química Inorgànica i Orgànica, Secció de Química Inorgànica, Universitat de Barcelona, E-08028 Barcelona, Spain; Institut de Nanociència i Nanotecnologia (IN2UB), Universitat de Barcelona, 08028 Barcelona, Spain;* orcid.org/0000-0003-1289-1587; Email: laura.rodriguez@qi.ub.es

J. Sérgio Seixas de Melo − *CQC, Department of Chemistry, University of Coimbra, 3004-535 Coimbra, Portugal;* orcid.org/0000-0001-9708-5079; Email: sseixas@ci.uc.pt

Authors

Andrea Pinto − *Departament de Química Inorgànica i Orgànica, Secció de Química Inorgànica, Universitat de Barcelona, E-08028 Barcelona, Spain; Institut de Nanociència i Nanotecnologia (IN2UB), Universitat de Barcelona, 08028 Barcelona, Spain*

Carla Cunha − *CQC, Department of Chemistry, University of Coimbra, 3004-535 Coimbra, Portugal*

Gabriel Aullón − *Departament de Química Inorgànica i Orgànica, Secció de Química Inorgànica, Universitat de Barcelona, E-08028 Barcelona, Spain; Institut de Química Teòrica i Computacional (IQTCUB), Universitat de Barcelona, 08028 Barcelona, Spain*

João Carlos Lima − *LAQV-REQUIMTE, Departamento de Química, Universidade Nova de Lisboa, 2829-516 Monte de Caparica, Portugal;* orcid.org/0000-0003-0528-1967

Complete contact information is available at: https://pubs.acs.org/10.1021/acs.jpcb.1c07985

Notes

The authors declare no competing financial interest.

ACKNOWLEDGMENTS

This work was supported by Project "Hylight" (No. 031625) 02/SAICT/2017, PTDC/QUI-QFI/31625/2017, which is funded by the Portuguese Science Foundation and Compete Centro 2020. We acknowledge funding by Fundo Europeu de Desenvolvimento Regional (FEDER) through Programa Operacional Factores de Competitividade (COMPETE). Centro de Química de Coimbra acknowledges the financial support of Fundação para a Ciência e Tecnologia for financial support (Projects UIDB/00313/2020 and UIDP/00313/2020). FCT is also acknowledged by Associated Laboratory for Green Chemistry, LAQV-REQUIMTE (UID/QUI/50006/2013). We acknowledge funding by Fundo Europeu de Desenvolvimento Regional (FEDER) through Programa Operacional Factores de Competitividade (COMPETE) and Project ROTEIRO/0152/2013. The authors are grateful to Spanish Ministerio de Ciencia e Innovación (Project PID2019-104121GB-I00). The research leading to these results has received funding from Laserlab-Europe (Grant Agreement No. 284464, EC's Seventh Framework Programme).

REFERENCES

(1) Vicente, J.; González-Herrero, P.; Pérez-Cadenas, M.; Jones, P. G.; Bautista, D. Synthesis, Structure, and Luminescence of Di-and Trinuclear Palladium/Gold and Platinum/Gold Complexes with (2, 7-Di-Tert-Butylfluoren-9-Ylidene) Methanedithiolate. *Inorg. Chem.* **2007**, *46*, 4718−4732.

(2) Meggers, E. Targeting Proteins with Metal Complexes. *Chem. Commun.* **2009**, 1001−1010.

(3) Au, V. K.-M.; Tsang, D. P.-K.; Wong, K. M.-C.; Chan, M.-Y.; Zhu, N.; Yam, V. W.-W. Functionalized Bis-Cyclometalated Alkynylgold (Iii) Complexes: Synthesis, Characterization, Electrochemistry, Photophysics, Photochemistry, and Electroluminescence Studies. *Inorg. Chem.* **2013**, *52*, 12713−12725.

(4) Yam, V. W.-W.; Cheng, E. C.-C. Highlights on the Recent Advances in Gold Chemistry—a Photophysical Perspective. *Chem. Soc. Rev.* **2008**, *37*, 1806−1813.

(5) Fernández, E. J.; Laguna, A.; López-de-Luzuriaga, J. M. Gold-Heterometal Complexes. Evolution of a New Class of Luminescent Materials. *Dalton Trans.* **2007**, 1969−1981.

(6) Pujadas, M.; Rodríguez, L. Luminescent Phosphine Gold (I) Alkynyl Complexes. Highlights from 2010 to 2018. *Coord. Chem. Rev.* **2020**, *408*, 213179.

(7) Paderina, A. V.; Koshevoy, I. O.; Grachova, E. V. Keep It Tight: A Crucial Role of Bridging Phosphine Ligands in the Design and Optical Properties of Multinuclear Coinage Metal Complexes. *Dalton Trans.* **2021**, *50*, 6003−6033.

(8) He, X.; Yam, V. W.-W. Luminescent Gold (I) Complexes for Chemosensing. *Coord. Chem. Rev.* **2011**, *255*, 2111−2123.

(9) Balch, A. L. Remarkable Luminescence Behaviors and Structural Variations of Two-Coordinate Gold (I) Complexes. *Struct. Bonding* **2007**, *123*, 1−40.

(10) Aguilo, E.; Moro, A. J.; Outis, M.; Pina, J.; Sarmento, D.; Seixas de Melo, J. S.; Rodríguez, L.; Lima, J. C. Deactivation Routes in Gold (I) Polypyridyl Complexes: Internal Conversion Vs Fast Intersystem Crossing. *Inorg. Chem.* **2018**, *57*, 13423−13430.

(11) Vogt, R. A.; Peay, M. A.; Gray, T. G.; Crespo-Hernández, C. E. Excited-State Dynamics of (Organophosphine) Gold (I) Pyrenyl Isomers. *J. Phys. Chem. Lett.* **2010**, *1*, 1205−1211.

(12) Vogt, R. A.; Gray, T. G.; Crespo-Hernandez, C. E. Subpicosecond Intersystem Crossing in Mono-and Di (Organophosphine) Gold (I) Naphthalene Derivatives in Solution. *J. Am. Chem. Soc.* **2012**, *134*, 14808−14817.

(13) Chan, K. T.; Tong, G. S. M.; To, W.-P.; Yang, C.; Du, L.; Phillips, D. L.; Che, C.-M. The Interplay between Fluorescence and Phosphorescence with Luminescent Gold (I) and Gold (Iii) Complexes Bearing Heterocyclic Arylacetylide Ligands. *Chem. Sci.* **2017**, *8*, 2352−2364.

(14) Belyaev, A.; Kolesnikov, I.; Melnikov, A. S.; Gurzhiy, V. V.; Tunik, S. P.; Koshevoy, I. O. Solution Versus Solid-State Dual Emission of the Au (I)-Alkynyl Diphosphine Complexes Via Modification of Polyaromatic Spacers. *New J. Chem.* **2019**, *43*, 13741−13750.

(15) Gutiérrez-Blanco, A.; Fernández-Moreira, V.; Gimeno, M. C. n.; Peris, E.; Poyatos, M. Tetra-Au (I) Complexes Bearing a Pyrene Tetraalkynyl Connector Behave as Fluorescence Torches. *Organometallics* **2018**, *37*, 1795−1800.

(16) Chia, Y.; Tay, M. An Insight into Fluorescent Transition Metal Complexes. *Dalton Trans.* **2014**, *43*, 13159−13168.

(17) Kondrasenko, I.; Chung, K.-y.; Chen, Y.-T.; Koivistoinen, J.; Grachova, E. V.; Karttunen, A. J.; Chou, P.-T.; Koshevoy, I. O. Harnessing Fluorescence Versus Phosphorescence Ratio Via Ancillary Ligand Fine-Tuned Mlct Contribution. *J. Phys. Chem. C* **2016**, *120*, 12196−12206.

(18) Goswami, S.; Winkel, R. W.; Schanze, K. S. Photophysics and Nonlinear Absorption of Gold (I) and Platinum (Ii) Donor-Acceptor-Donor Chromophores. *Inorg. Chem.* **2015**, *54*, 10007−10014.

(19) Longevial, J. F.; El Cheikh, K.; Aggad, D.; Lebrun, A.; van der Lee, A.; Tielens, F.; Clément, S.; Morère, A.; Garcia, M.; Gary-Bobo, M.; Richeter, S. Porphyrins Conjugated with Peripheral Thiolato Gold(I) Complexes for Enhanced Photodynamic Therapy. *Chem.—Eur. J.* **2017**, *23*, 14017−14026.

(20) Uçüncü, M.; Karakuş, E.; Kurulgan Demirci, E.; Sayar, M.; Dartar, S.; Emrullahoğlu, M. Bodipy-Au (I): A Photosensitizer for Singlet Oxygen Generation and Photodynamic Therapy. *Org. Lett.* **2017**, *19*, 2522−2525.

(21) Ogilby, P. R. Singlet Oxygen: There Is Indeed Something New under the Sun. *Chem. Soc. Rev.* **2010**, *39*, 3181−3209.
(22) Forward, J. M.; Bohmann, D.; Fackler Jr, J. P.; Staples, R. J. Luminescence Studies of Gold (I) Thiolate Complexes. *Inorg. Chem.* **1995**, *34*, 6330−6336.
(23) Arcau, J.; Andermark, V.; Aguiló, E.; Gandioso, A.; Moro, A.; Cetina, M.; Lima, J. C.; Rissanen, K.; Ott, I.; Rodríguez, L. Luminescent Alkynyl-Gold (I) Coumarin Derivatives and Their Biological Activity. *Dalton Trans.* **2014**, *43*, 4426−4436.
(24) Rampazzi, V.; Roger, J.; Amardeil, R.; Penouilh, M.-J.; Richard, P.; Fleurat-Lessard, P.; Hierso, J.-C. Gold (I) Complexes of Ferrocenyl Polyphosphines: Aurophilic Gold Chloride Formation and Phosphine-Concerted Shuttling of a Dinuclear [Clau··· Aucl] Fragment. *Inorg. Chem.* **2016**, *55*, 10907−10921.
(25) Moro, A. J.; Rome, B.; Aguiló, E.; Arcau, J.; Puttreddy, R.; Rissanen, K.; Lima, J. C.; Rodríguez, L. A Coumarin Based Gold (I)-Alkynyl Complex: A New Class of Supramolecular Hydrogelators. *Org. Biomol. Chem.* **2015**, *13*, 2026−2033.
(26) Gil-Rubio, J.; Camara, V.; Bautista, D.; Vicente, J. Dinuclear Alkynyl Gold (I) Complexes Containing Bridging N-Heterocyclic Dicarbene Ligands: New Synthetic Routes and Luminescence. *Organometallics* **2012**, *31*, 5414−5426.
(27) Pinto, A.; Hernández, G.; Gavara, R.; Aguiló, E.; Moro, A. J.; Aullón, G.; Malfois, M.; Lima, J. C.; Rodríguez, L. Supramolecular Tripodal Au (I) Assemblies in Water. Interactions with a Pyrene Fluorescent Probe. *New J. Chem.* **2019**, *43*, 8279−8289.
(28) Seixas de Melo, J.; Becker, R. S.; Elisei, F.; Maçanita, A. The Photophysical Behavior of 3-Chloro-7-Methoxy-4-Methylcoumarin Related to the Energy Separation of the Two Lowest-Lying Singlet Excited States. *J. Chem. Phys.* **1997**, *107*, 6062−6069.
(29) Seixas de Melo, J. S.; Becker, R. S.; Maçanita, A. L. Photophysical Behavior of Coumarins as a Function of Substitution and Solvent: Experimental Evidence for the Existence of a Lowest Lying 1 (N. Pi.*) State. *J. Phys. Chem.* **1994**, *98*, 6054−6058.
(30) Assefa, Z.; McBurnett, B. G.; Staples, R. J.; Fackler, J. P.; Assmann, B.; Angermaier, K.; Schmidbaur, H. Syntheses, Structures, and Spectroscopic Properties of Gold (I) Complexes of 1, 3, 5-Triaza-7-Phosphaadamantane (Tpa). Correlation of the Supramolecular Au. Cntdot. Cntdot. Cntdot. Au Interaction and Photoluminescence for the Species (Tpa) Aucl and [(Tpa-Hcl) Aucl]. *Inorg. Chem.* **1995**, *34*, 75−83.
(31) Garcia-Vergara, S.; Habazaki, H.; Skeldon, P.; Thompson, G. Formation of Porous Anodic Alumina at High Current Efficiency. *Nanotechnology* **2007**, *18*, 415605.
(32) Tian, Y.; Liang, Z.; Xu, H.; Mou, Y.; Guo, C. Design, Synthesis and Cytotoxicity of Novel Dihydroartemisinin-Coumarin Hybrids Via Click Chemistry. *Molecules* **2016**, *21*, 758.
(33) Seixas de Melo, J. S. The Influence of Oxygen on the Lifetime of Luminescent Probes. A Simple Device for Degassing Solutions for Fluorescence Measurements. *Chem. Educ.* **2005**, *10*, 29−35.
(34) Seixas de Melo, J. S.; Pina, J.; Dias, F. B.; Maçanita, A. L. Experimental Techniques for Excited State Characterisation. In *Applied Photochemistry*; Springer, 2013; pp 533−585.
(35) Kristiansen, M.; Scurlock, R. D.; Iu, K. K.; Ogilby, P. R. Charge-Transfer State and Singlet Oxygen (1. Delta. G O2) Production in Photoexcited Organic Molecule-Molecular Oxygen Complexes. *J. Phys. Chem.* **1991**, *95*, 5190−5197.
(36) Pina, J.; Seixas de Melo, J.; Burrows, H.; Maçanita, A.; Galbrecht, F.; Bunnagel, T.; Scherf, U. Alternating Binaphthyl-Thiophene Copolymers: Synthesis, Spectroscopy, and Photophysics and Their Relevance to the Question of Energy Migration Versus Conformational Relaxation. *Macromolecules* **2009**, *42*, 1710−1719.
(37) Striker, G.; Subramaniam, V.; Seidel, C. A.; Volkmer, A. Photochromicity and Fluorescence Lifetimes of Green Fluorescent Protein. *J. Phys. Chem. B* **1999**, *103*, 8612−8617.
(38) Frisch, M. J.; Trucks, G. W.; Schlegel, H. B.; Scuseria, G. E.; Robb, M. A.; Cheeseman, J. R.; Scalmani, G.; Barone, V.; Mennucci, B.; Petersson, G. A.; et al. *Gaussian 09*, revision B.1; Gaussian Inc.: Wallingford, CT, 2010.
(39) Becke, A. Density-Functional Thermochemistry. Iii. The Role of Exact Exchange. *J. Chem. Phys.* **1993**, *98*, 5648.
(40) Lee, C.; Yang, W.; Parr, R. G. Development of the Colle-Salvetti Correlation-Energy Formula into a Functional of the Electron Density. *Phys. Rev. B: Condens. Matter Mater. Phys.* **1988**, *37*, 785.
(41) Weigend, F.; Ahlrichs, R. Balanced basis sets of split valence, triple zeta valence and quadruple zeta valence quality for H to Rn: Design and assessment of accuracy. *Phys. Chem. Chem. Phys.* **2005**, *7*, 3297−3305.
(42) Schäfer, A.; Horn, H.; Ahlrichs, R. Fully Optimized Contracted Gaussian Basis Sets for Atoms Li to Kr. *J. Chem. Phys.* **1992**, *97*, 2571−2577.
(43) Reed, A. E.; Curtiss, L. A.; Weinhold, F. Intermolecular Interactions from a Natural Bond Orbital, Donor-Acceptor Viewpoint. *Chem. Rev.* **1988**, *88*, 899−926.
(44) Casida, M. E.; Jamorski, C.; Casida, K. C.; Salahub, D. R. Molecular Excitation Energies to High-Lying Bound States from Time-Dependent Density-Functional Response Theory: Characterization and Correction of the Time-Dependent Local Density Approximation Ionization Threshold. *J. Chem. Phys.* **1998**, *108*, 4439−4449.
(45) García-Moreno, E.; Gascón, S.; Rodriguez-Yoldi, M. J.; Cerrada, E.; Laguna, M. S-Propargylthiopyridine Phosphane Derivatives as Anticancer Agents: Characterization and Antitumor Activity. *Organometallics* **2013**, *32*, 3710−3720.
(46) Gavara, R.; Aguiló, E.; Schur, J.; Llorca, J.; Ott, I.; Rodríguez, L. Study of the Effect of the Chromophore and Nuclearity on the Aggregation and Potential Biological Activity of Gold (I) Alkynyl Complexes. *Inorg. Chim. Acta* **2016**, *446*, 189−197.
(47) Andermark, V.; Goke, K.; Kokoschka, M.; Abu el Maaty, M. A.; Lum, C. T.; Zou, T.; Sun, R. W.-Y.; Aguilo, E.; Oehninger, L.; Rodriguez, L.; Bunjes, H.; Wolfl, S.; Che, C.-M.; Ott, I. Alkynyl Gold (I) Phosphane Complexes: Evaluation of Structure-Activity-Relationships for the Phosphane Ligands, Effects on Key Signaling Proteins and Preliminary in-Vivo Studies with a Nanoformulated Complex. *J. Inorg. Biochem.* **2016**, *160*, 140−148.

https://doi.org/10.1021/acs.jpcb.1c07985
J. Phys. Chem. B XXXX, XXX, XXX−XXX